INTERACTION AND MERGING OF CUSPATE FORELANDS FORMED AT END OF MULTIPLE SANDY ISLANDS UNDER WAVES

Shiho Miyahara[1],Takaaki Uda [2] and Masumi Serizawa[1]

The shapes of the cuspate forelands formed at the end of multiple sandy islands were investigated, taking seven islands in Korea, Japan, and Russia as examples. When two sandy islands are located successively, the cuspate foreland formed at the end of one island deforms while being subjected to the wave-sheltering effect of the other island. In this study, the BG model (a model for predicting three-dimensional beach changes based on Bagnold's concept) was used to predict the topographic changes when waves were incident randomly to the two islands in the downward and upward directions, and the interaction and merging of the cuspate forelands formed at the end of multiple sandy islands were investigated.

Keywords: sandy islands; interaction; merging; wave-sheltering effect; BG model

INTRODUCTION

When waves are incident from two opposite directions in a shallow sea, a land-tied island or a cuspate foreland may develop. Miyahara et al. (2014) carried out the field observations of the land-tied island, Yoshima Island located offshore of Shodoshima Island in the Seto Inland Sea and Chiringashima Island located at the entrance of Kagoshima Bay. Then, a model for predicting the behavior of a land-tied island was developed using the BG model (a model for predicting three-dimensional beach changes based on Bagnold's concept) (Serizawa et al. 2006). Furthermore, Serizawa et al. (2015) studied the morphological features of Futtsu cuspate foreland in Japan and a cuspate foreland located at the northeast end of Graham Island in British Colombia, Canada, and developed a new model for predicting the formation of a cuspate foreland using the BG model under the condition that waves were incident from two opposite directions. In their study, the wave field was predicted using the energy balance equation for irregular waves (Mase 2001), including the effect of wave refraction and wave breaking, as well as the wave-sheltering effect of the cuspate foreland itself. The BG model was further applied to the prediction of beach changes for the case of multiple islands. Serizawa et al. (2014) carried out a numerical simulation of the deformation of multiple circular islands composed of sand in a shallow sea. In their calculation, the deformation of two circular islands was predicted when waves were incident from all directions between 0° and 360° with the same probability, taking the wave-sheltering effect of one island on the other island into account. Under real conditions, there are many cases of multiple islands deforming while interacting with each other. In this study, beach changes associated with the interaction and merging of the cuspate forelands formed at the end of two sandy islands were investigated using the BG model when waves were incident from completely opposite directions, and each cuspate foreland was subject to the wave-sheltering effect of another island.

INTERACTION OF CUSPATE FORELANDS FORMED AT END OF MULTIPLE ISLANDS

In the central part of the islands facing the Yellow Sea in southwest Korea, an example of cuspate forelands formed at the end of islands that interact with each other can be seen. Figure 1 shows a satellite image of multiple islands as an example. Figure 2 is an enlarged image of the multiple islands (34°44'03.53" N, 126°02'33.24" E) distributed within the rectangular area shown in Fig. 1. A shallow sea where a tidal flat can develop extends around the islands, and islands A, B, and C are located in order from the west. Island B is east of island A separated by a strait of 200 m width, and island C is located southeast of island B. These two islands are connected each other via a slender sandbar of 200 m length. This sandbar has a symmetric shape with respect to its centerline. Although another cuspate foreland extends at the east end of island A, it extends toward island B with a tip that curves southward. Similarly, a sand spit with a tip curving northward is formed at the west end of island B. These sand spits are assumed to have elongated while being subject to the wave-sheltering effect from the other island, although the effect alters with the distance between the islands and the size of the islands.

The second example is the cuspate foreland connecting two islands located at 34°55'10" N and 126°10'09" E in the south part of Korea facing the Yellow Sea (Fig. 3). Originally, there were three islands with the largest one on the west, and an island with smaller size on the east together with another island in the middle of the cuspate foreland. These islands were connected each other by a

[1] Coastal Engineering Laboratory Co., Ltd., 1-22-301 Wakaba, Shinjuku, Tokyo 160-0011, Japan
[2] Public Works Research Center, 1-6-4 Taito, Taito, Tokyo 110-0016, Japan

sandbar, and the sandbar was pulled northward at the central part by the wave-sheltering effect of the islands in the middle of the cuspate foreland.

The third example is the cuspate foreland on Bijindo Island located at 34°43'10" N and 128°27'46" E offshore of Busan in Korea, as shown in Fig. 4. In this case, two islands are connected each other by a slender, symmetric cuspate foreland, implying that waves with an equivalent energy are incident from both sides of the cuspate foreland. Similar cases can be seen in the Seto Inland Sea in Japan. Figure 5 shows the cuspate foreland on Yuri-jima Island, which is located at 33°51'04" N and 132°31'34" E in the Seto Inland Sea. Originally, there existed two islands, and they were connected each other by a sharp cuspate foreland. Because of the smaller size of west island, the size of cuspate foreland is smaller on the west side. Figure 6 shows the cuspate foreland extending between Hashira-jima and Tsuzuki-shima Islands located at 34°00'36" N and 132°25'41" E in the Seto Inland Sea, and a sharp

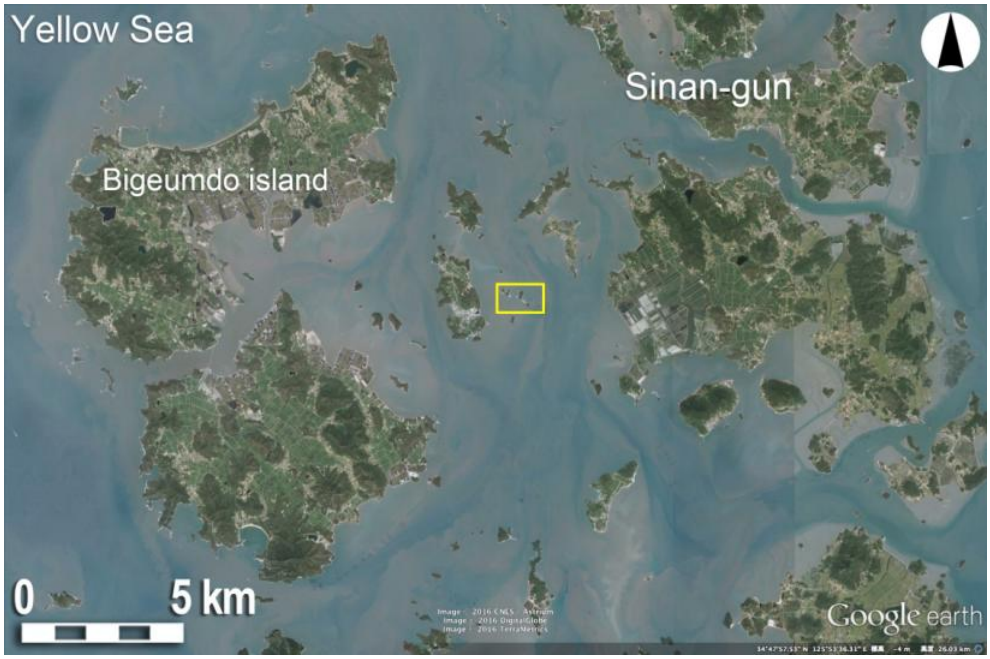

Figure 1. Satellite image of islands facing the Yellow Sea in southwestern Korea.

Figure 2. Cuspate forelands extending from islands and connected with each other.

cuspate foreland extends southeast to the wave-shelter zone of Tsuzuki-shima Island. Apart from this, at the north end of Tsuzuki-shima Island, a small cuspate foreland extends to the NNW direction

paralell to the cuspate foreland extending from the southeast end of Hashira-jima Island. Figure 7 shows the cuspate foreland extended on Oshima Island located at 34°22'35" N and 133°35'10" E in the Seto Inland Sea. Originally, Oshima Island was also composed of two islands connected by a slender cuspate foreland with 100 m length. The shape of the sandbar between the islands is very similar to the case of Bijindo Island in Korea, as shown in Fig. 4.

The seventh example is the multiple islands located 45 km offshore of the coast facing the Kara Sea in Russia (Zenkovich, 1967, Fig. 252, p. 509). Figure 8 shows a satellite image of these islands. Islands A and B are separated by a strait of 3.5 km width, whereas a wide strait of 9.3 km length separates island B from island C. The cuspate forelands are seemed to be extended from both ends of islands A and B, as if they are attracting each other. It is seen from the satellite image that a triangular lowland is formed at the east end of island A. In contrast, a slender cuspate foreland with the tip curved southwestward is formed at the west end of island B. Furthermore, two recurved sand spits with a lagoon inside extend from the east end of island B because the width of the strait is large between islands B and C, and stronger waves could be incident to the east end of island B. In this study, the development of these cuspate forelands formed at the end of the multiple islands and the successive deformation of the sandbar formed by the connection of the cuspate forelands were numerically simulated using the BG model given a simple calculation condition.

Figure 3. Cuspate foreland around an island located in south part of Korea.

Figure 4. Cuspate foreland on Bijindo Island offshore of Busan in Korea.

Figure 5. Cuspate foreland on Yuri-jima Island in the Seto Inland Sea, Japan.

Figure 6. Cuspate forelands extending between Hashira-jima and Tsuzuki-shima Islands.

Figure 7. Cuspate foreland extended on Oshima Island.

Figure 8. Cuspate foreland formed at tips of multiple islands in Kara Sea.

CALCULATION METHOD

For the sand transport flux, Eq. (1) of the BG model was employed, the same fundamental equation as in Serizawa et al. (2014), and is equal to the Type 4 BG model in Uda et al. (2018).

$$\vec{q} = C_0 \frac{P}{\tan\beta_c} \left\{ \begin{array}{l} K_n\left(\tan\beta_c \vec{e_w} - |\cos\alpha| \vec{\nabla Z}\right) \\ + \left\{ (K_s - K_n)\sin\alpha - \dfrac{K_2}{\tan\bar{\beta}} \dfrac{\partial H}{\partial s} \right\} \tan\beta \vec{e_s} \end{array} \right\} \qquad (1)$$

$$(-h_c \le Z \le h_R)$$

Here, $\vec{q} = (q_x, q_y)$ is the net sand transport flux for the total sediment transport, Z (x, y, t) is the elevation of the seabed to be determined, and n and s are the local coordinates taken in the direction normal to the contour line (shoreward positive) and parallel to the contour line, respectively. $\vec{\nabla Z} = (\partial Z/\partial x,\ \partial Z/\partial y)$ is the slope vector, $\vec{e_w}$ is the unit vector for the wave direction, $\vec{e_s}$ is the unit vector taken in the direction parallel to the contour line, α is the angle between the wave direction and the direction normal to the contour line, and $|\cos\alpha| = \left|\vec{e_w} \bullet \vec{\nabla Z}\right| \Big/ \left|\vec{\nabla Z}\right|$. $\tan\beta = \left|\vec{\nabla Z}\right|$ is the seabed slope. $\tan\beta_c$ is the equilibrium slope, which mainly depends on the grain size of the bed materials, $\tan\beta\ \vec{e_s} = (-\partial Z/\partial y,\ \partial Z/\partial x)$, and K_s and K_n are the coefficients of longshore and cross-shore sand transport, respectively. K_2 is the coefficient of Ozasa and Brampton's term, and $\partial H/\partial s = \vec{e_s} \cdot \vec{\nabla H}$ is the longshore gradient of H measured parallel to the contour line. $\tan\bar{\beta}$ is the seabed slope in the surf zone. C_0 is the coefficient through which the sand transport rate, expressed in terms of the immersed weight, is related to the volumetric sand transport rate ($C_0 = 1/\{(\rho_s - \rho)g(1-p)\}$; ρ is the specific weight of seawater, ρ_s is the specific weight of a sand particle, p is the porosity of sand, g is the acceleration of gravity), and h_c and h_R are the depth of closure and berm height, respectively.

For the P value in Eq. (1), the wave dissipation rate at each point owing to wave breaking, Φ_{all}, which can be determined by the calculation of the planar wave field, was employed.

$$P = \Phi_{all} \qquad (2)$$

For the calculation of the wave field, the energy balance equation of Mase (2001) was employed with the term of wave decay due to wave breaking (Dally et al. 1984) to take the effects of wave refraction and the decay of irregular waves due to the wave breaking and wave-sheltering effect of the cuspate forelands themselves into account. Φ_{all} in Eq. (2) was calculated from Eq. (3), and is the total energy dissipation by the breaking of each component wave.

$$\Phi_{all} = f_D E = K\sqrt{g/h}\left[1 - (\Gamma/\gamma)^2\right]E \qquad (P \ge 0) \qquad (3)$$

Here, f_D is the wave dissipation rate, E is the wave energy, K is a coefficient expressing the intensity of wave decay due to breaking, h is the water depth, Γ is the ratio of the wave height at the breaking point relative to the water depth on a flat seabed, and γ is the ratio of the wave height to the water depth H/h. In the calculation, Φ_{all} calculated from Eq. (3) was employed as the P value using wave energy E, which was determined in the calculation process of the wave field.

An imaginary depth was set in the wave run-up area. The wave energy was assumed to be 0 at a location where the elevation was higher than the berm height. The beach changes were calculated from the continuity equation by the explicit finite difference method given the sand transport flux of Eq. (1) using a staggered mesh scheme. On the slope of the island with a high elevation where direct wave action does not reach, slope failure occurs when the slope exceeds that of the repose angle of sand. In this case, downslope movement of sand is forced to occur. The wave field was recurrently calculated every 10 steps in the calculation of beach changes. Further detail of the calculation method can be found in Uda et al. (2018).

CALCULATION CONDITIONS

Cartesian coordinates (x, y) were selected, and a rectangular area with 1.2 and 4.0 km length in the x- and y-directions, respectively, was selected as the calculation domain (Fig. 9). The water depth was assumed to be 4 m, and two sandy islands of an obelisk and symmetrical with respect to the center of the calculation domain O were set. The reason why the two islands were arranged symmetrically was so the wave-sheltering effect of one island could reach the other island. Because the islands had an obelisk shape, the shoreline of the square islands had a side of 200 m length. A sandy beach with a berm height of 1 m and an initial beach slope of 1/20 was assumed on a solid seabed, together with an obelisk-shape sand supply source with 31 m height and 1/2 slope, as shown in Fig. 10. The reason for selecting the arrangement of the high obelisk as the sand source was that a sufficient volume of sand for the elongation of the sandbar could be supplied. If this amount of sand were small, the cuspate forelands would not extend sufficiently. Although the initial shoreline shape was given as square in this study, the initial shape could be given as any shape. Waves with a height of 1 m and wave period of 4 s were incident from the upper and lower boundaries of the calculation domain with the same probability of 0.5. Regarding the wave incidence from two directions, the wave direction was selected every 10 steps of the calculation of beach changes using random numbers. Table 1 summarizes the calculation conditions. The calculation was carried out up to 12,010 steps.

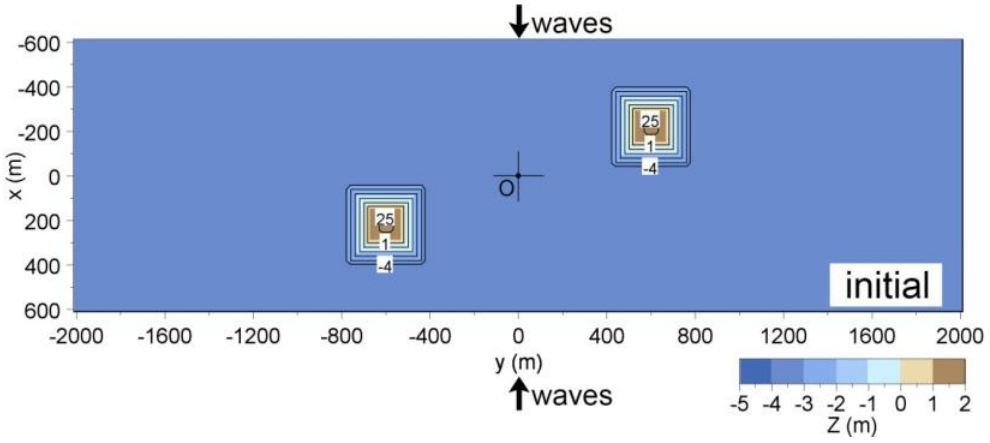

Figure 9. Initial shape of two islands of obelisk shape.

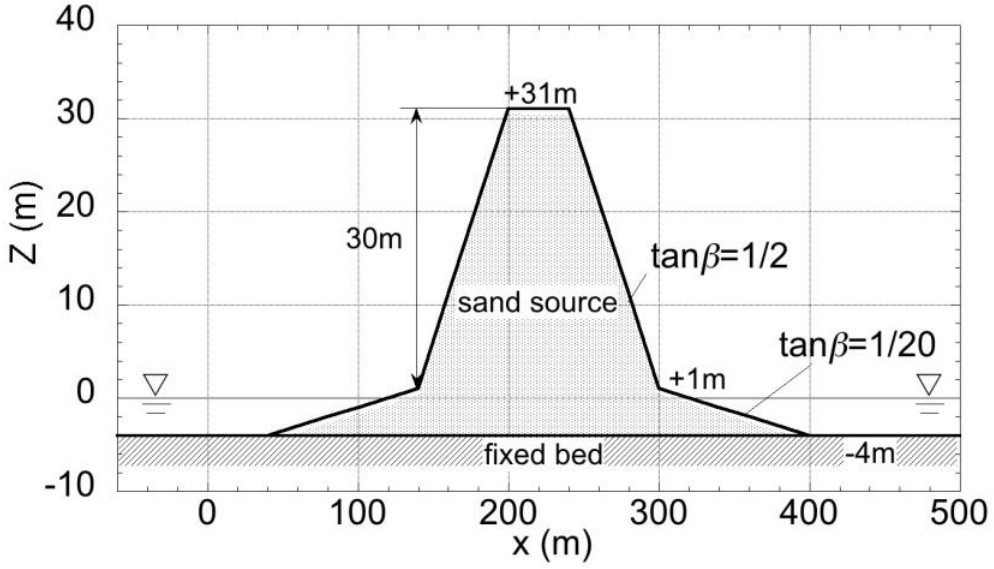

Figure 10. Crosssection of sandy islands.

Table 1. Calculation conditions.	
Wave conditions	Incident waves: H_I = 1 m, T = 4 s, wave direction θ_I = 0° and 180° relative to -x axis
Berm height	h_R = 1 m
Depth of closure	h_c = 4 m
Equilibrium slope	tanβ_c = 1/20
Coefficients of sand transport	Coefficient of longshore sand transport K_s = 0.2 Coefficient of Ozasa and Brampton (1980) term K_2=1.62K_s Coefficient of cross-shore sand transport K_n = K_s
Mesh size	Δx = Δy = 20 m
Time intervals	Δt = 0.5 h
Duration of calculation	6.0005 × 10^3 hr (1.201×10^4 steps)
Boundary conditions	Shoreward and landward ends: q_x = 0, right and left boundaries: q_y = 0
Calculation of wave field	Energy balance equation (Mase 2001) • Term of wave dissipation due to wave breaking: Dally et al. (1984) model • Wave spectrum of incident waves: directional wave spectrum density obtained by Goda (1985) • Total number of frequency components N_F = 1 and number of directional subdivisions N_θ = 8 • Directional spreading parameter S_{max} = 25 • Coefficient of wave breaking K = 0.17 and Γ = 0.3 • Imaginary depth between minimum depth h_0 (0.5 m) and berm height h_R • Wave energy = 0 where $Z \geq h_R$ • Lower limit of h in terms of wave decay due to breaking: 0.5 m

CALCULATION RESULTS

For waves with the same probability randomly incident from the ±x-directions to these sandy islands, the calculation results up to 12,000 steps are shown in Fig. 11. The cuspate forelands started to elongate from both ends of the sandy islands toward the y-axis and become a flatter shape owing to the action of the waves incident from the ±x-axis directions after 2,000 steps. The cuspate forelands extending between the islands approached each other after 4,000 steps. After 6,000 steps, the slender cuspate forelands extending from the ends of the two islands were almost connected to each other, resembling shaking hands. After 8,000 steps, the two islands were connected to each other and a

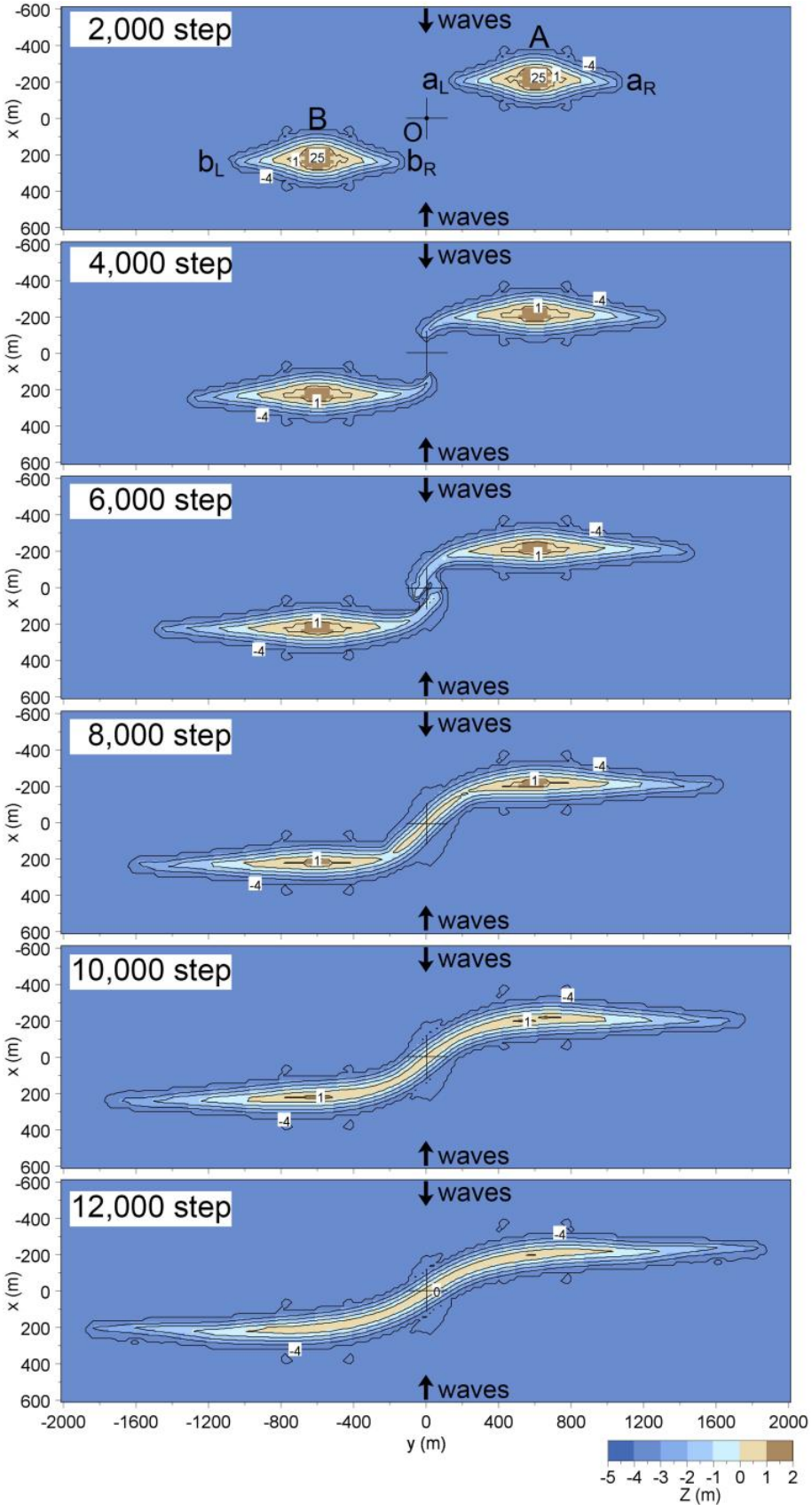

Figure 11. Calculation results of connection of two islands.

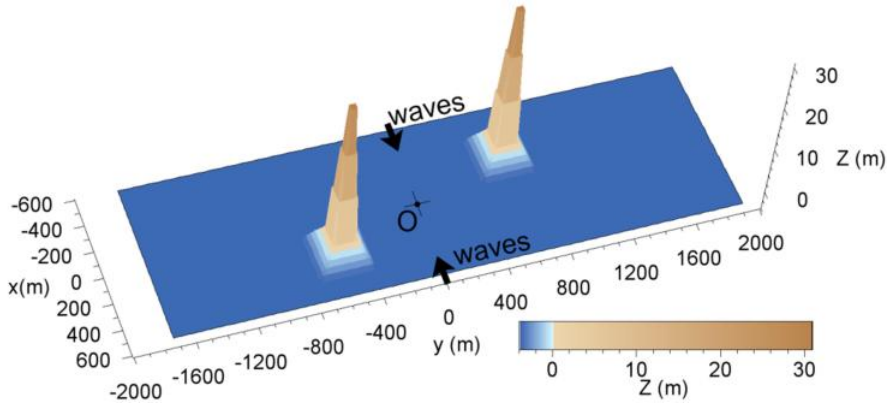

Figure 12. Bird's-eye figure of initial topography.

smooth shoreline was formed. With time, the connecting sandbar between the two islands further deformed and elongated in such a manner that the longshore gradient of the shoreline gradually decreased in the vicinity of point O. After 12,000 steps, a slender sandbar appeared, and a single slender island was formed. The formation of a connecting sandbar (Fig. 2) between islands B and C in the Yellow Sea in southwest Korea is similar to the calculation results after 8,000 steps in Fig. 11, and the shape of the cuspate forelands formed at the end of islands A and B in the Kara Sea (Fig. 8) is assumed to be at a primitive stage of the extention of cuspate forelands after 4,000 steps, as shown in Fig. 11.

The calculation results are better shown using bird's-eye figure instead of the contour line expression, because a large vertical change in the elevation of the islands took place, associated with the slope failure. Figure 12 shows the initial shape, where the vertical scale is expanded compared with that of the horizontal scale. At the initial stage, two islands with a high peak existed. When waves were incident to these islands from the upper and lower boundaries with the same probability, the islands continued to change, as shown in Fig. 13. With time, the islands with a high peak were rapidly eroded, resulting in the decrease in the height, and the high peaks disappeared by 10,000 steps.

In order to investigate the change in the wave field around the cuspate forelands and the resultant sandbar, the right and left islands are designated as islands A and B, respectively, as shown in Fig. 11. Furthermore, the cuspate forelands at the left and right ends of islands A and B are designated as a_L and a_R, and b_L and b_R, respectively. Using these designations, the wave fields after 2,000 and 2,010 steps with waves incident from the upper and lower boundaries, respectively, are shown in Fig. 14. At this stage, the wave-shelter zone is independently formed behind each slender island in response to the change in the wave direction. Even though waves are incident from the upper or lower boundary, the wave-shelter zone behind island A (B) does not reach island B (A), and the cuspate forelands formed at the end of the island extend only in the transverse direction with no interaction between the islands because of the symmetric wave field.

When waves are incident from the upper boundary after 4,000 steps, as shown in Fig. 15, waves are incident to the cuspate foreland a_L at the left end of island A without the wave-sheltering effect from island B, whereas waves affected by the wave-sheltering effect of a_L are incident to the cuspate foreland b_R at the right end of island B. When waves are incident from the reverse direction, waves affected by the wave-sheltering effect of b_R are incident to a_L of island A. When superimposing the actions of waves propagating downward and upward onto a_L, downward wave action prevails, forcing the tip of the cuspate foreland to bend downward, and vice versa at b_R. As a result, a_L bends downward, whereas b_R bends upward, while approaching each other. Thus, the tip of the cuspate foreland formed at the end of each island extends to the wave-shelter zone formed by the other island, and both tips of the cuspate forelands approach each other. In contrast, a_R and b_L extend in the transverse direction because there is no wave-sheltering effect from the other island.

The cuspate forelands a_L and b_R approach each other after 6,000 steps by the same mechanism, as shown in Fig. 16, and the cuspate forelands almost join each other after 6,000 and 6,020 steps, creating a wide wave-shelter zone together with wave intrusion through the vicinity of point O. After 8,000 and 12,000 steps, wave invasion across the sandbar near point O ceases because of sufficient elongation of the sandbar, and only waves diffracted from the ends of the connected sandbar propagate to the lee of

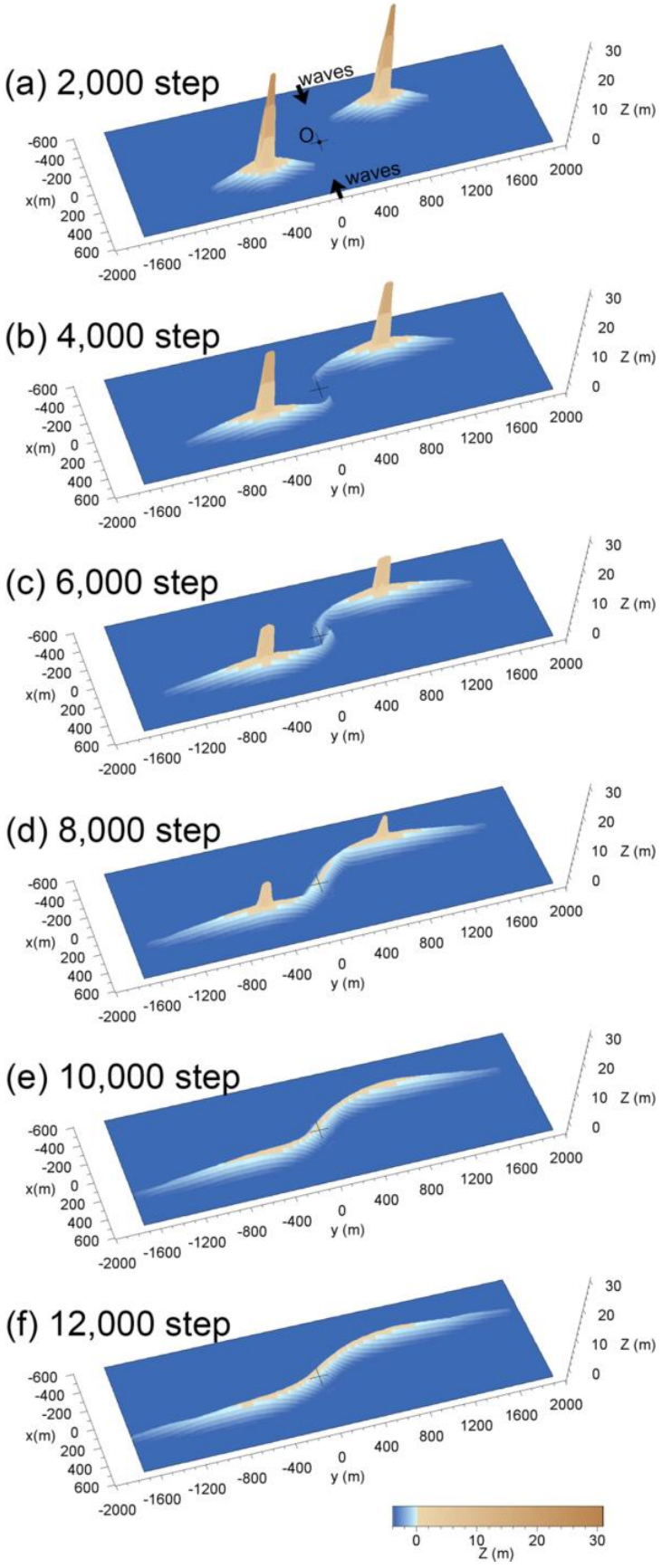

Figure 13. Bird's-eye figure of beach changes during the connection of cuspate forelands.

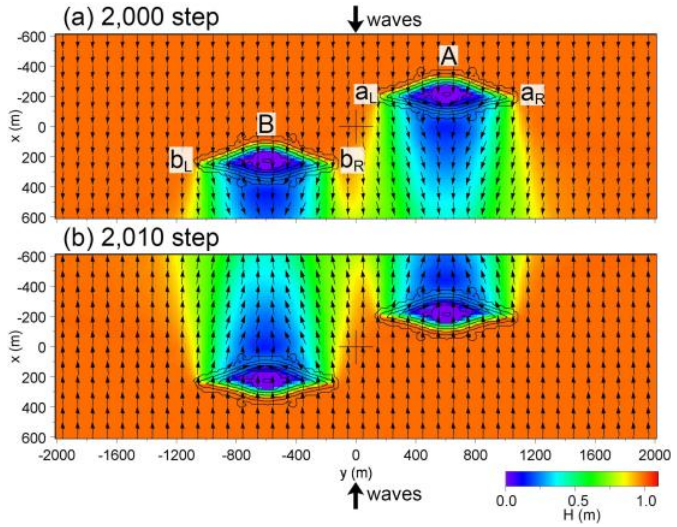

Figure14. Wave fields after 2,000 and 2,010 steps.

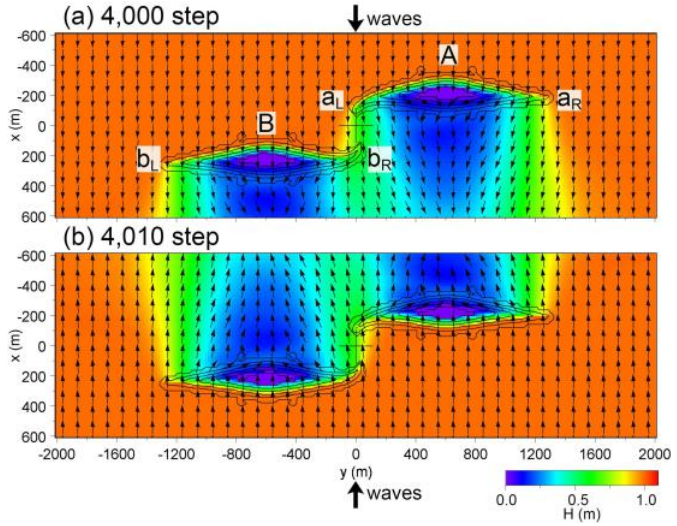

Figure 15. Wave fields after 4,000 and 4,010 steps.

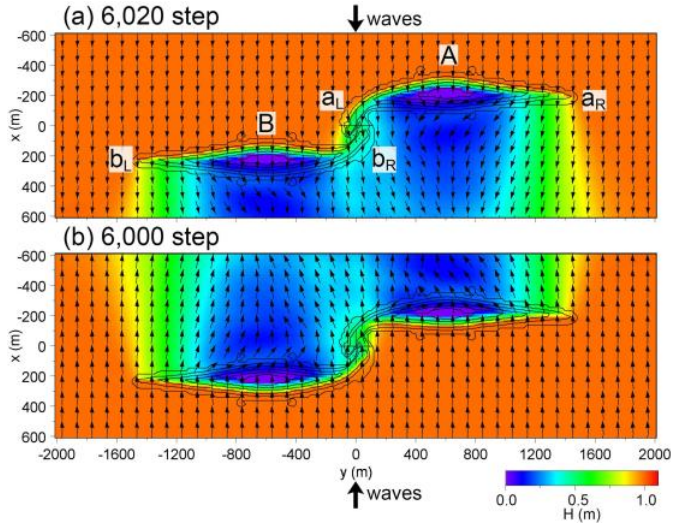

Figure 16. Wave fields after 6,000 and 6,020 steps.

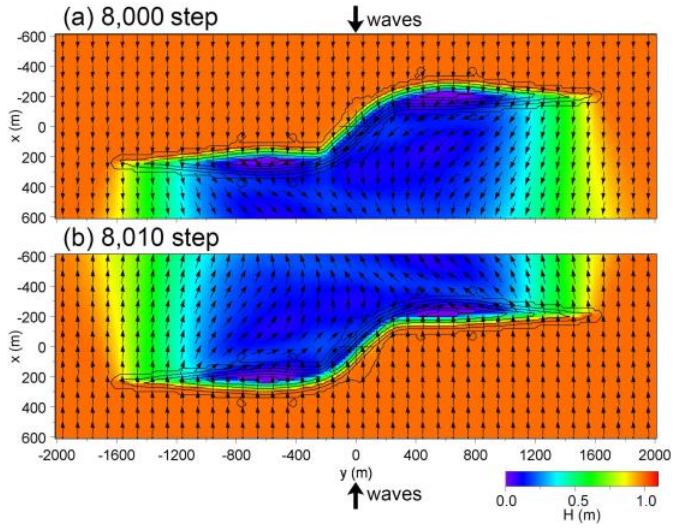

Figure 17. Wave fields after 8,000 and 8,010 steps.

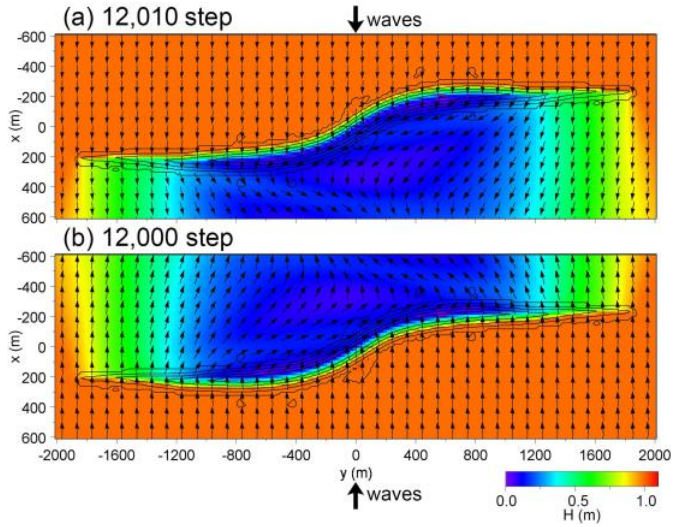

Figure 18. Wave fields after 12,000 and 12,020 steps.

the connected sandbar, as shown in Figs. 17 and 18. Under this condition, leftward sand transport flux is induced in the central part of the sandbar because the shoreline inclination is large when waves are incident from the upper boundary in the downward direction, whereas rightward sand transport is induced when waves are incident from the lower boundary in the upward direction because the action of the diffracted waves can be neglected.

The net sand transport flux corresponding to the wave fields at five stages is shown in Fig. 19. After 2,000 steps, sand transport flux occurs around each of the two sandy islands, rendering them a slender form. Between 4,000 and 8,000 steps, the two islands further extend with a greater sand transport flux in the central part of the islands because of the large shoreline inclination. Then, the sand transport flux declines because the shoreline inclination decreases with time. At the same time, both tips of each sandy island extend while maintaining a slender form. Thus, for the development of a cuspate foreland from an island, the need for a sufficient amount of sand exists and, at the same time, waves must be incident from two opposite directions. In addition, the wave-sheltering effect of one island on the other island is a neccesary condition for the cuspate forelands formed at the end of two islands to connect and merge with each other. Finally, it can be concluded that the BG model can be successfully used for predicting the interaction and merging of multiple sandy islands separated by a certain distance.

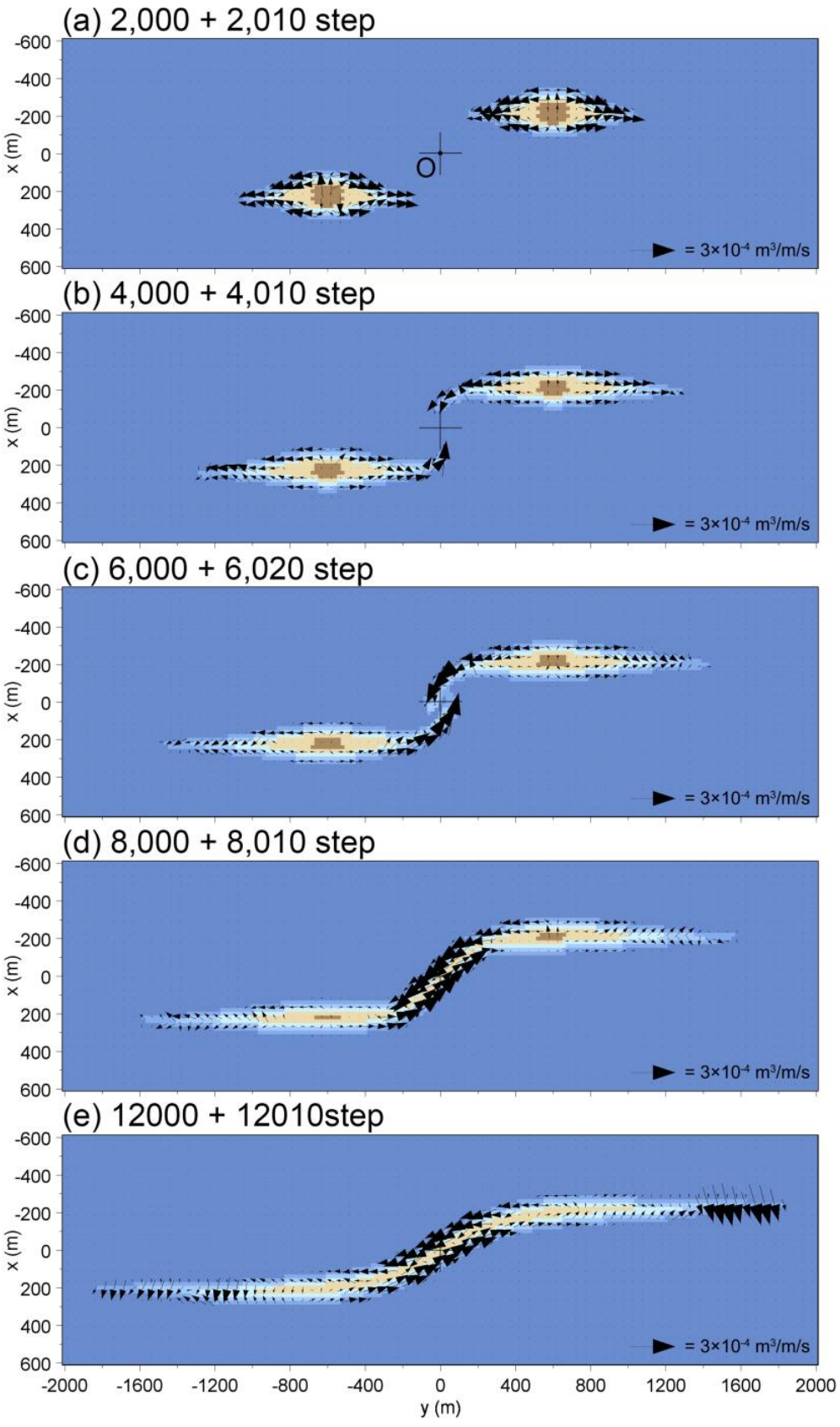

Figure 19. Net sand transport fluxes at five stages.

CONCLUSIONS

Multiple islands in Korea, Japan, and Russia were taken as examples of the deformation of cuspate forelands formed at the tips of multiple islands that interact with each other. The topographic changes associated with the interaction and merging of sandbars were investigated under the conditions that multiple sandy islands were located successively, and cuspate forelands extending from the end of the islands were subject to the wave-sheltering effect of the other island. The BG model was applied to predict the beach changes of multiple islands when waves were incident from the upper and lower boundaries with the same probability. The mechanism of beach changes associated with interaction and merging of multiple islands was successfully explained by the numerical simulation.

REFERENCES

Dally, W.R., R.G. Dean and R.A. Dalrymple. 1984. A model for breaker decay on beaches, *Proceedings of 19th International Conference on Coastal Engineering*, ASCE, 82-97.

Goda, Y. 1985. *Random Seas and Design of Maritime Structures*, University of Tokyo Press, Tokyo, 323 pp.

Mase, H. 2001. Multidirectional random wave transformation model based on energy balance equation, *Coastal Eng. J.*, JSCE, 43(4), 317-337.

Miyahara, S., T. Uda, and M. Serizawa. 2014. Prediction of formation of land-tied islands, *Proceedings of 34th International Conference on Coastal Engineering*, ASCE, 1-14.

Ozasa, H., and A.H. Brampton. 1980. Model for predicting the shoreline evolution of beaches backed by seawalls, *Coastal Eng.,* 4, 47-64.

Serizawa, M., T. Uda, T. San-nami, and K. Furuike. 2006. Three-dimensional model for predicting beach changes based on Bagnold's concept, *Proceedings of 30th International Conference on Coastal Engineering*, ASCE, 3155-3167.

Serizawa, M., T. Uda, and S. Miyahara. 2014. Interaction between two circular sandy islands on flat shallow seabed owing to waves, *Proceedings of 34th International Conference on Coastal Engineering*, ASCE, 1-12.

Serizawa, M., T. Uda, and S. Miyahara. 2015. Model for predicting formation of a cuspate foreland, *Coastal Sediments '15*, 65, 1-14.

Uda, T., M. Serizawa, and S. Miyahara. 2018. *Morphodynamic model for predicting beach changes based on Bagnold's concept and its applications*, INTEC, London, UK.
Doi: http://dx.doi.org/10.5772/intechopen.81411

Zenkovich, V.P. 1967. *Processes of Coastal Development*, Interscience Publishers, New York, 751pp.